AIAA JOURNAL
Vol. 36, No. 9, September 1998

Adaptive Shape Control of Laminated Composite Plates Using Piezoelectric Materials

S. Varadarajan,* K. Chandrashekhara,† and S. Agarwal‡
University of Missouri–Rolla, Rolla, Missouri 65409

Shape control of laminated composite plates with integrated piezoelectric actuators is discussed. The effectiveness of piezoelectric actuators and position sensors is investigated for shape control under the influence of quasistatically varying unknown loads. The shape control problem is divided into two parts. 1) For the desired shape function, calculate initial actuator input voltages such that a measure of the mean-squared error between the desired and the achieved shape is minimized. 2) An adaptive feedback algorithm is developed so as to minimize the distortion in the shape introduced by the quasistatically varying loads on the structure. A finite element model based on the shear deformation theory is used to verify the performance of the shape control methodologies.

Introduction

SMART structures incorporating integrated piezoelectric sensors and actuators have found a wide range of applications in the fields of active vibration control, shape control, and noise suppression. Most of the research in this field has, however, been directed toward vibration control problems. In many applications precise and automatic shape control of the structure is important. Piezoelectric actuators could, for example, be used to adjust the shape and, hence, the focal length of space antennas. Another application of shape control is to improve the performance of an aerodynamic or hydrodynamic lifting surface.

A general method is developed to study adaptive shape control of laminated composite plates with piezoelectric actuators. The effectiveness of the piezoelectric actuators and position sensors is investigated for the shape control problem. A finite element model based on first-order shear deformation theory is used to verify the performance of the shape control design.

Many researchers have addressed the issues of mathematical modeling of laminated composite plates with piezoelectric materials, including Lee,[1] Crawley and Lazarus,[2] Wang and Rogers,[3] and Chandrashekhara and Agarwal.[4] Shape control of nitinol-reinforced composite beams was studied by Baz et al.[5] The mathematical model developed describes the interaction between the shape memory effect of the composite beams and the thermally induced shape memory effect of the nitinol strips. Austin et al.[6] presented analytical and experimental studies on static shape control of adaptive wings by employing internal translational actuators. The changes in shape of sandwich plates and shells with embedded piezoelectric actuators has been reported by Koconis et al.[7]

The aim of the present paper is to study the shape control problem where the structure is subjected to quasistatically varying unknown loads. Thus, the transient vibration is neglected. Moreover, the time-varying unknown loads are assumed to be small such that the distortion in the shape introduced due to these unknown loads is small. An appropriate error function is defined as a measure of difference between the desired and the achieved shape. Shape control is achieved in two steps. With the assumption that the external loads are known and are constant, an initial set of actuator input voltages is obtained by a constrained minimization of the error function. An adaptive feedback control is then incorporated to maintain the desired shape in the presence of quasistatically varying loads. It is assumed that a position sensor is available at each node for feedback.

Presented as Paper 96-1288 at the AIAA/ASME/AHS Adaptive Structures Forum, Salt Lake City, UT, April 18–19, 1996; received Aug. 12, 1996; revision received March 7, 1998; accepted for publication May 8, 1998. Copyright © 1998 by the American Institute of Aeronautics and Astronautics, Inc. All rights reserved.

*Graduate Research Assistant, Department of Mechanical and Aerospace Engineering and Engineering Mechanics.
†Professor, Department of Mechanical and Aerospace Engineering and Engineering Mechanics. Associate Fellow AIAA.
‡Graduate Research Assistant, Department of Electrical Engineering.

Mathematical Model

A laminated plate with integrated piezoelectric actuators, as shown in Fig. 1, is considered. The actuators can be bonded or embedded within the laminated plate, and each actuator can be independently actuated. The stress–strain relationships, accounting for transverse shear deformation and piezoelectric effect, can be expressed as[4]

$$\begin{Bmatrix}\sigma_x\\ \sigma_y\\ \tau_{yz}\\ \tau_{xz}\\ \tau_{xy}\end{Bmatrix}_k = \begin{bmatrix}Q_{11} & Q_{12} & 0 & 0 & Q_{16}\\ Q_{12} & Q_{22} & 0 & 0 & Q_{26}\\ 0 & 0 & Q_{44} & Q_{45} & 0\\ 0 & 0 & Q_{45} & Q_{55} & 0\\ Q_{16} & Q_{26} & 0 & 0 & Q_{66}\end{bmatrix}_k \times \left(\begin{Bmatrix}\epsilon_x\\ \epsilon_y\\ \gamma_{yz}\\ \gamma_{xz}\\ \gamma_{xy}\end{Bmatrix}_k - \begin{bmatrix}0 & 0 & d_{31}\\ 0 & 0 & d_{31}\\ 0 & d_{15} & 0\\ d_{15} & 0 & 0\\ 0 & 0 & 0\end{bmatrix}_k \begin{Bmatrix}0\\ 0\\ E_3\end{Bmatrix}_k \right) \tag{1}$$

where Q_{ij} are the transformed elastic coefficients and d_{ij} are the piezoelectric coefficients. The electric field intensity E_3^k is given by

$$E_3^k = v_3^k / h_k \tag{2}$$

where v_3^k is the applied voltage across the kth layer and h_k is the thickness of the kth layer.

The strains in Eq. (1) are related to the displacements as follows:

$$\epsilon_x = \epsilon_x^0 + z\kappa_x, \qquad \epsilon_y = \epsilon_y^0 + z\kappa_y$$
$$\gamma_{xy} = \gamma_{xy}^0 + z\kappa_{xy}, \qquad \gamma_{yz} = \gamma_{yz}^0, \qquad \gamma_{xz} = \gamma_{xz}^0 \tag{3}$$

where

$$\epsilon_x^0 = \frac{\partial u}{\partial x}, \qquad \epsilon_y^0 = \frac{\partial v}{\partial y}, \qquad \gamma_{xy}^0 = \frac{\partial u}{\partial y} + \frac{\partial v}{\partial x}$$
$$\kappa_x = \frac{\partial \phi_x}{\partial x}, \qquad \kappa_y = \frac{\partial \phi_y}{\partial y}, \qquad \kappa_{xy} = \frac{\partial \phi_x}{\partial y} + \frac{\partial \phi_y}{\partial x} \tag{4}$$
$$\gamma_{yz}^0 = \phi_y + \frac{\partial w}{\partial y}, \qquad \gamma_{xz}^0 = \phi_x + \frac{\partial w}{\partial x}$$

In Eq. (4), u, v, and w are the midplane displacements and ϕ_x and ϕ_y are the normal rotations.

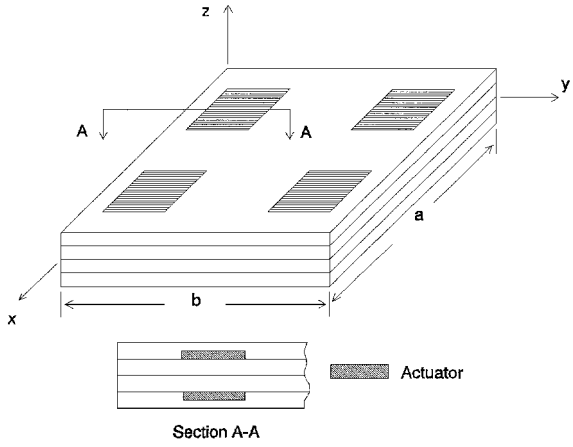

Fig. 1 Laminated composite plate with integrated piezoelectric actuators.

Finite Element Formulation

The mathematical statement of the principle of virtual work can be expressed as

$$\int_v \delta(U^* - W^*)\,\mathrm{d}V = 0 \tag{5}$$

where U^* is the strain energy and W^* is the work done by the prescribed surface tractions.

The generalized displacements in any element can be expressed as

$$\{u(x, y)\} = \sum_{i=1}^{n} \left[N_i^e(x, y)\right]\left\{u_i^e\right\} \tag{6}$$

where

$$\left[N_i^e\right] = N_i^e[I], \qquad \left\{u_i^e\right\} = (u_i, v_i, w_i, \phi_{xi}, \phi_{yi})^t$$

where n is the number of nodes; N_i^e are the element shape functions; $[I]$ is a 5×5 identity matrix; and u_i, v_i, w_i, ϕ_{xi}, and ϕ_{yi} are the nodal values of u, v, w, ϕ_x, and ϕ_y, respectively.

Using Eqs. (5) and (6), the element equations can be written as

$$[K]^e\{\Delta\}^e = \{\boldsymbol{f}\}^e_{\text{ex}} + \{\boldsymbol{g}\}^e v^e \tag{7}$$

where $[K]^e$ is the element stiffness matrix, $\{\Delta\}^e$ is the nodal displacement vector, $\{\boldsymbol{f}\}^e_{\text{ex}}$ is the element force vector due to external loading, $\{\boldsymbol{g}\}^e$ is the element piezoelectric force vector per unit voltage, and v^e is the voltage applied to the piezoelectric actuator.

Assembling Eq. (7) and treating each distributed actuator as independent, we get

$$[K]\{\Delta\} = \{\boldsymbol{f}\}_{\text{ex}} + [G]\{\boldsymbol{V}\}_{\text{ac}} \tag{8}$$

where $\{\Delta\}$ is a $(5n \times 1)$ vector of nodal displacements, $[K]$ is a $(5n \times 5n)$ global stiffness matrix, $\{\boldsymbol{f}\}_{\text{ex}}$ is a $(5n \times 1)$ force vector, $[G]$ is a $(5n \times p)$ matrix, n is the number of nodes, and p is the number of independent actuators.

Applying the boundary conditions to Eq. (8), the nodal displacements can be obtained as

$$\{\Delta\} = [\bar{K}]^{-1}[\{\bar{\boldsymbol{f}}\}_{\text{ex}} + [\bar{G}]\{\boldsymbol{V}\}_{\text{ac}}] \tag{9}$$

where $[\bar{K}]$ and $[\bar{G}]$ and $\{\bar{\boldsymbol{f}}\}_{\text{ex}}$ are the condensed matrices and force vector, respectively.

Shape Control

The shape of the plate is described by the transverse displacement w at any location (x, y). Let the desired shape function for the plate be given by

$$w = \xi(x, y) \tag{10}$$

where w is the desired transverse displacement at location (x, y) on the plate. Also it is assumed that $\xi(x, y)$ is continuous and differentiable in the domain.

To quantify the error in the achieved shape of the structure as compared to the desired shape, an error function is defined as the sum of the squared difference between the achieved and the desired transverse displacement at the nodal points δ_i. Thus,

$$J = \sum_{i=1}^{n} \delta_i^2 = \sum_{i=1}^{n} [\xi_i - w_i]^2 \tag{11}$$

where w_i is the actual transverse displacement at the ith node and ξ_i is the corresponding desired displacement. Because of the shear and axial displacement, the transverse displacement w_i is actually measured at $(x_i + u_i, y_i + v_i)$, where u_i and v_i are the axial displacements at the ith node. Thus, using simple geometric reasoning, the nodal error can be expressed as[7]

$$\delta_i = \xi(x_i, y_i) - \left[w_i - \left(\frac{\partial \xi}{\partial x}\right)_i u_i - \left(\frac{\partial \xi}{\partial y}\right)_i v_i\right] \tag{12}$$

The shape error function J defined in Eq. (11) can then be expressed in terms of the nodal error vector $(\boldsymbol{\Lambda})$ as

$$J = \boldsymbol{\Lambda}^T \boldsymbol{\Lambda} \tag{13}$$

where the nodal error vector $\boldsymbol{\Lambda}$ is given by

$$\boldsymbol{\Lambda} = \begin{Bmatrix} \delta_1 \\ \vdots \\ \delta_n \end{Bmatrix} = \{\boldsymbol{W}\}_d - [\{\boldsymbol{W}\}_{FE} - [\Delta W_x]_d\{\boldsymbol{U}\}_{FE} - [\Delta W_y]_d\{\boldsymbol{V}\}_{FE}] \tag{14}$$

where $\{\boldsymbol{W}\}_d$ is the vector corresponding to desired transverse displacement at the nodes; $[\Delta W_x]_d$ and $[\Delta W_y]_d$ are $n \times n$ diagonal matrices whose diagonal terms are the slopes $(d\xi/dx)_i$ and $(d\xi/dy)_i$ of the desired shape function $\xi(x, y)$; and $\{\boldsymbol{U}\}_{FE}$, $\{\boldsymbol{V}\}_{FE}$, and $\{\boldsymbol{W}\}_{FE}$ are the axial and transverse nodal displacement vectors. Using Eq. (9), the axial and transverse nodal displacement vectors $\{\boldsymbol{U}\}_{FE}$, $\{\boldsymbol{V}\}_{FE}$, and $\{\boldsymbol{W}\}_{FE}$ can be expressed as

$$\{\boldsymbol{U}\}_{FE} = [K_u]\{\Delta\} \tag{15a}$$

$$\{\boldsymbol{V}\}_{FE} = [K_v]\{\Delta\} \tag{15b}$$

$$\{\boldsymbol{W}\}_{FE} = [K_w]\{\Delta\} \tag{15c}$$

where $[K_u]$, $[K_v]$, and $[K_w]$ are $(n \times 4n)$ transformation matrices of zeros and ones that extract the axial and transverse displacements from $\{\Delta\}$.

The nodal error vector in Eq. (14) can be written as

$$\boldsymbol{\Lambda} = \{\boldsymbol{W}\}_d - [EF]\{\bar{\boldsymbol{f}}\}_{\text{ex}} - [RS]\{\boldsymbol{V}\}_{\text{ac}} \tag{16a}$$

where

$$[EF] = ([K_w] - [\Delta W_x]_d[K_u] - [\Delta W_y]_d[K_v])[\bar{K}]^{-1} \tag{16b}$$

$$[RS] = [EF][\bar{G}] \tag{16c}$$

Having defined the error function, the shape control can be defined as the problem to obtain an optimal set of actuator voltages $\{\boldsymbol{V}\}_{\text{ac}}$ such that the quadratic error function J as defined by Eq. (13) is minimized. Furthermore, the actuator voltages should satisfy the constraint that

$$v_{\min} < v_i < v_{\max} \tag{17}$$

where v_i is the input voltage to the ith actuator and $v_{\min}$ and $v_{\max}$ are the lower and upper saturation voltages of the actuator. In general, $v_{\min}$ and $v_{\max}$ for each actuator may be different. However, in the present work it is assumed that all of the actuators have the same lower and upper saturation voltages.

From Eq. (16) it can be noted that the nodal error vector and, hence, the shape error function J are dependent on the external loading $\{\bar{\boldsymbol{f}}\}_{\text{ex}}$. Even though a nominal value of these external loads may be known, they may not be accurate. In practical conditions, this external loading changes over time due to various factors. This

variation can, however, be assumed to be quasistatic so that the transient vibrations due to the time-varying load can be neglected. Thus, the external load can be decomposed into a known nominal load $\{f_0\}_{ex}$ and an unknown quasistatically varying load $\{f_u(t)\}_{ex}$. For quasistatically varying loads, a two-stage solution to the shape control problem is proposed.

1) First is open-loop shape control. With the assumption that the external load is known, $\{f_u(t)\}_{ex} = 0$, the optimum actuator voltages can be obtained directly by solving the constrained least-squares problem. Because it does not need any kind of feedback, it has been called *open-loop control*. Note at this point that, even though the shape achieved with open-loop control is close to the desired shape, it may not be the same. Thus, the shape of the structure achieved by open-loop control is referred to as *open-loop shape*. For the given actuator placements and given nominal external loads, open-loop shape is the best achievable shape that is closest to the desired shape in the least-square sense.

2) Next is closed-loop shape control. In the presence of small time-varying loads, the distortions in shape that are introduced due to these unknown loads should be corrected for. This can be achieved through an adaptive feedback control algorithm. Feedback is called *adaptive* because the feedback gain matrix changes as the individual actuators go into saturation.

In the following two subsections open-loop shape control and closed-loop shape control problems are discussed in more detail.

Open-Loop Shape Control

Because the external load is assumed to be known precisely in this case, the nodal error vector can be written as

$$\Lambda = \{W'\}_d - [RS]\{V\}_{ac} \tag{18a}$$

where

$$\{W'\}_d = \{W\}_d - [EF]\{\bar{f}_0\}_{ex} \tag{18b}$$

The error function J is the sum of the squared errors at the nodal points of the plate. Thus, a set of actuator voltages $\{V\}_{ac}$ that minimizes J in fact also minimizes the error between the desired shape and the achieved shape and is, thus, optimal in the mean-squared-error sense. Moreover, the optimal set of actuator voltages can be obtained by a minimization of the error function J in Eq. (13) under the constraints given by Eq. (17).

The constrained optimization problem is solved using the Lagrange multiplier approach. For a structure with p actuators, there are $2p$ different constraints on actuator voltages ($v_i > v_{min}$, $i = 1, \ldots, p$, and $v_i < v_{max}$ for $i = 1, \ldots, p$). Thus, an augmented cost function H can be defined as

$$H = \Lambda^T\Lambda + \sum_{i=1}^{p} \lambda_i^1 (v_i - v_{min})^2 + \sum_{i=1}^{p} \lambda_i^2 (v_{max} - v_i)^2 \tag{19}$$

Equation (19) can also be expressed as

$$H = \Lambda^T\Lambda + \{V - V_{min}\}^T \lambda^1 \{V - V_{min}\} + \{V_{max} - V\}^T \lambda^2 \{V_{max} - V\} \tag{20}$$

where λ^1 and λ^2 are the diagonal matrices formed with Lagrange multipliers λ_i^1 and λ_i^2, respectively, and $\{V\}$ is the vector of actuator voltages. According to the theory of Lagrange multipliers, the problem of determining the actuator voltage $\{V\}$ that minimizes Eq. (13) subject to the constraints in Eq. (17) can be obtained by minimizing the augmented cost function H without any constraints. The augmented cost function H is minimized with respect to the actuator voltages and the Lagrange multipliers λ^1 and λ^2. The Lagrange multipliers λ_i^1 and λ_i^2 take values of zero or one, and both λ_i^1 and λ_i^2 are not one at the same time. Note that a nonzero value for the Lagrange multiplier implies that the corresponding actuator is constrained at the maximum or the minimum actuator voltage. A nonzero value for λ_i^1 implies that the ith actuator should have $v_i = v_{min}$, and a nonzero value for λ_i^2 implies that the ith actuator should have $v_i = v_{max}$. If both λ_i^1 and λ_i^2 are zeros, the corresponding actuator is said to be unconstrained. The input voltages for the unconstrained actuators can be obtained by a least-square minimization of a truncated error function $\bar{J} = \bar{\Lambda}^T\bar{\Lambda}$, where

$$\bar{\Lambda} = \{\bar{W}\}_d - [\overline{RS}]\{\bar{V}\}_{ac} \tag{21}$$

where $\{\bar{W}\}_d$ and $[\overline{RS}]$ are obtained by dropping appropriate rows and columns corresponding to the constrained actuators. The linear system, Eq. (21), is solved to obtain the vector of actuator voltages $\{\bar{V}\}_{ac}$ as

$$\{\bar{V}\}_{ac} = ([\overline{RS}]^T[\overline{RS}])^{-1}[\overline{RS}]^T\{\bar{W}\}_d \tag{22}$$

The actual actuator voltages $\{V\}_{ac}$ are obtained by appending suitable values for the constrained actuators. Thus,

$$v_i = \begin{cases} v_{min} & \text{if} \quad v_i < v_{min} \left(\lambda_i^1 \neq 0, \lambda_i^2 = 0\right) \\ v_{max} & \text{if} \quad v_i > v_{max} \left(\lambda_i^1 = 0, \lambda_i^2 \neq 0\right) \\ v_i & \text{otherwise} \left(\lambda_i^1 = 0, \lambda_i^2 = 0\right) \end{cases} \tag{23}$$

In the preceding development it is assumed that the constraints on the actuators are known a priori. However, that is never the case. In the present work, an iterative algorithm is used to systematically obtain the constraints on the actuators and, thus, to obtain an optimal set of actuator voltages.

1) To start, assume all actuators are unconstrained.

2) Obtain the truncated set of actuator voltages $\{\bar{V}\}_{ac}$ by dropping all of the constrained actuators, using Eq. (22).

3) Obtain the optimal actuator voltages $\{V\}_{ac}$ using Eq. (23).

4) If all of the actuator voltages satisfy the constraints in Eq. (17), the solution is implied; else, suitably constrain the actuators for which the constraints are violated.

5) Continue from step 2.

Closed-Loop Shape Control

In the preceding section, input actuator voltages were calculated to achieve a desired shape in the presence of known external loading. Most practical structures such as aerodynamic wings or space structures are subjected to quasistatic unknown loads due to temperature changes or other external stimuli during the course of their operation. These loads tend to distort the achieved shape of the structure. The closed-loop shape control problem involves finding a set of correction voltages for the actuator input based on the difference between the desired and the achieved outputs at the sensor locations, so as to maintain the shape of the structure. In the present discussion position sensors have been assumed.

The finite element equations for a plate with piezoelectric actuators, given by Eq. (17), in the presence of unknown external loads, can be written as

$$[\bar{K}]\{\Delta\}_u = \{\bar{f}_0\}_{ex} + \{\bar{f}_u(t)\}_{ex} + [\bar{G}]\{V\}_{ac} \tag{24}$$

where $\{\bar{f}_u(t)\}_{ex}$ is the force vector because of unknown external loads on the structure. The new error vector can be written as

$$\Lambda_u = \{W\}_d - [EF]\{\{\bar{f}\}_u + \{\bar{f}\}_{ex}\} - [RS]\{V\}_{ac} \tag{25}$$

The sensor measurement for position sensor at given nodal points is given by

$$\{Y\}_s = [S][EF]\{\{\bar{f}\}_u + \{\bar{f}\}_{ex}\} + [S][RS]\{V\}_{ac} \tag{26}$$

where $[S]$ is the sensor matrix that consists of zeros and ones so that each row has only one nonzero entry corresponding to the sensor location.

The desired sensor output is given by

$$\{Y\}_d = [S]\{W\}_d \tag{27}$$

The aim of closed-loop feedback control is to minimize the error between the actual and the desired sensor outputs:

$$\bar{\Lambda}_u = [S]\Lambda_u = \{Y\}_d - \{Y\}_s \tag{28}$$

A schematic of closed-loop shape control, as shown in Fig. 2, is implemented. The actuator voltage is given by

$$\{V(i+1)\}_{ac} = \{V(i)\}_{ac} + \{\Delta V\}_{ac} \tag{29}$$

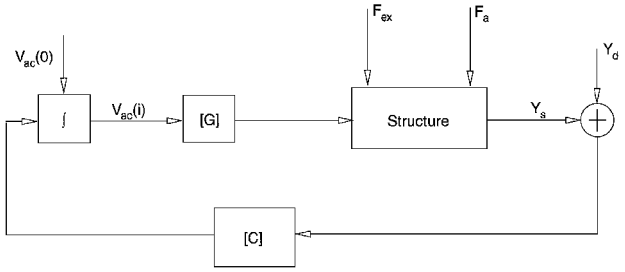

Fig. 2 Block diagram of the closed-loop system.

where $\{\Delta V\}_{ac}$ is the incremental input voltage and $\{V(i-1)\}_{ac}$ is the initial actuator voltage.

Thus, the aim is to calculate the control law

$$\{\Delta V\}_{ac} = [C]\{\{Y\}_d - \{Y\}_s\} \tag{30}$$

so that the sensor error function

$$J_u = \bar{\Lambda}_u^T \bar{\Lambda}_u \tag{31}$$

is minimized. The matrix $[C]$ in Eq. (30) represents the feedback gain.

Using Eq. (28) in Eq. (31), J_u is minimized by

$$\{\Delta V\}_{ac} = [([S][RS])^T([S][RS])]^{-1}([S][RS])^T[\{Y\}_d - \{Y\}_s] \tag{32}$$

The feedback gain matrix can be expressed as

$$[C] = [([S][RS])^T([S][RS])]^{-1}([S][RS])^T \tag{33}$$

The distortion ratio γ is defined as the ratio between the mean-squared error of the final shape to that of the initial shape and is given by

$$\gamma = J/J_0 \tag{34}$$

Results and Discussion

Numerical results are presented for open-loop and closed-loop shape control of laminated plates with integrated piezoelectric actuators using a nine-noded isoparametric element. For simplicity, a four-layer symmetric cross-ply [0/90/90/0]-deg laminated plate with one layer of piezoceramic patch bonded on top and bottom surfaces is considered. The thickness of the piezoceramic patch is taken as 2×10^{-4} m, and the actuator voltage limit is assumed as $-200 < v_i < 200$ V for all of the examples considered. The material properties considered for T300/5208 graphite/epoxy are $E_{11} = 181.0$ GPa, $E_{22} = 10.3$ GPa, $G_{12} = G_{13} = 7.17$ GPa, $G_{23} = 6.21$ GPa, and $\nu_{12} = 0.25$ and for PZT G1195 piezoceramic are $E = 63$ GPa, $\nu = 0.31$, and $d_{31} = d_{32} = -166 \times 10^{-12}$ m/V.

Open-Loop Shape Control

A laminated plate strip ($a = 0.5$ m, $b = 0.1$ m, and $h = 2.54 \times 10^{-3}$ m), with actuator configuration as shown in Fig. 3, is considered to study the static shape control problem. The plate strip is modeled using 24 elements. The desired and achieved shapes of the plate strip with clamped-free boundary conditions ($u = v = w = \phi_x = \phi_y = 0$ at $x = 0, a$) are shown in Fig. 4. The actuator voltage limit is taken as $-200 < v_i < 200$ V. The desired deflection is assumed as $w_d = 0.25[1 - \cos(\pi x/a)]$ in millimeters, where $a = 500$ mm. The actuator voltages and the distortion ratio are given in Table 1. It is observed that none of the constraints is applied because all of the actuator voltages are within the specified range. Figure 5 shows the desired and achieved shapes of the plate strip with clamped-clamped boundary conditions ($u = v = w = \phi_x = \phi_y = 0$ at $x = 0, a$). The actuator voltage limit is taken as $-250 < v_i < 250$ V. The desired shape is assumed as $w_d = 0.025[1 - \cos(4\pi x/a)]$ in millimeters. The actuator voltages and distortion ratio for this problem are also shown in Table 1. Note that, at the optimal solution, the constraints $v_2 = v_5 = 250$ V are active.

Closed-Loop Shape Control

A laminated plate with simply supported (SS) boundary conditions ($u = w = \phi_y = 0$ at $x = 0, a$ and $v = w = \phi_x = 0$ at $y = 0, b$), with actuator configuration as shown in Fig. 6, is considered. The

Table 1 Actuator voltages and distortion ratios

Actuator voltages, V	Figure 4	Figure 5
v_1	105.35	−133.14
v_2	−172.03	250
v_3	−38.29	−124.87
v_4	42.56	−124.87
v_5	155.57	250
v_6	110.98	−133.14
Distortion ratio	1.104×10^{-4}	3.733×10^{-2}

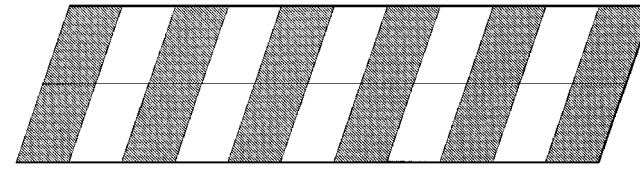

Fig. 3 Layout of plate strip with actuators.

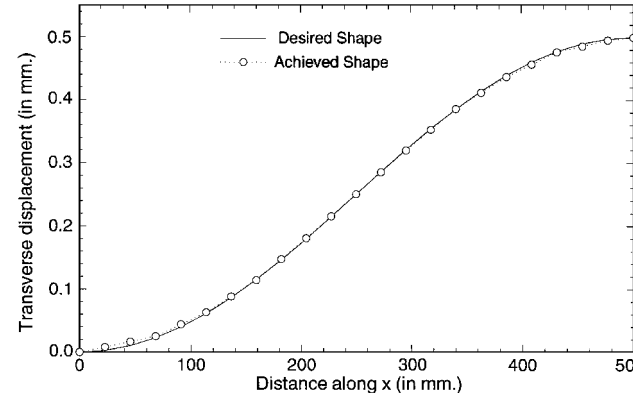

Fig. 4 Desired and achieved shapes for a plate strip with clamped-free edges.

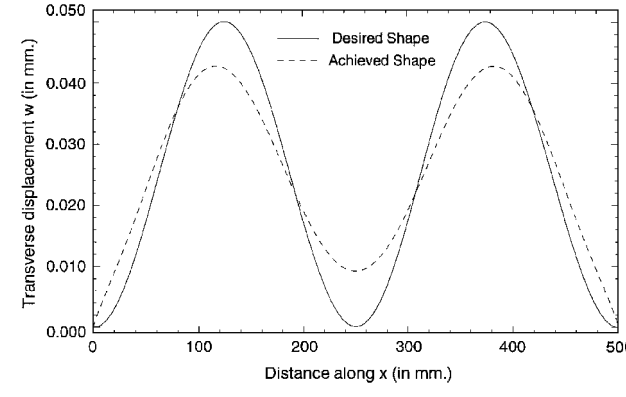

Fig. 5 Desired and achieved shapes for a plate strip with clamped-clamped edges.

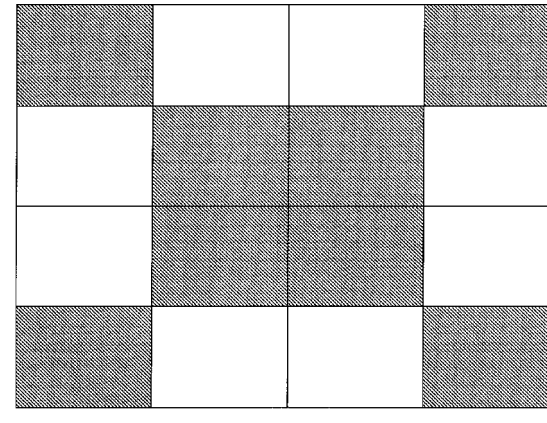

Fig. 6 Layout of rectangular plate with actuators.

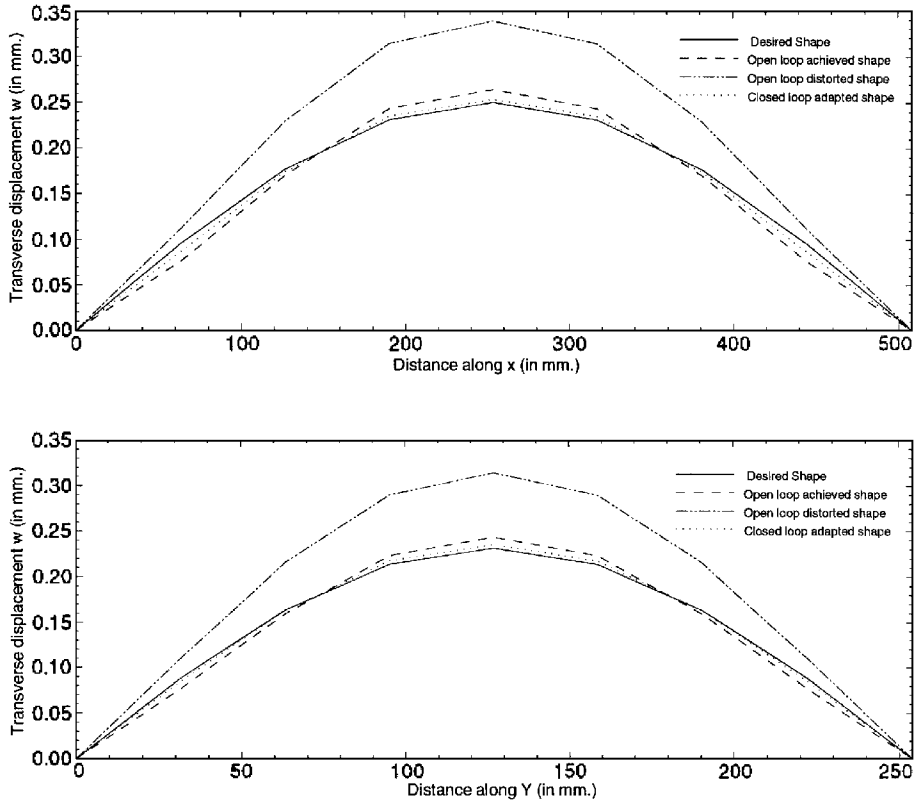

Fig. 7 Open-loop achieved and closed-loop adapted shapes for an SS plate.

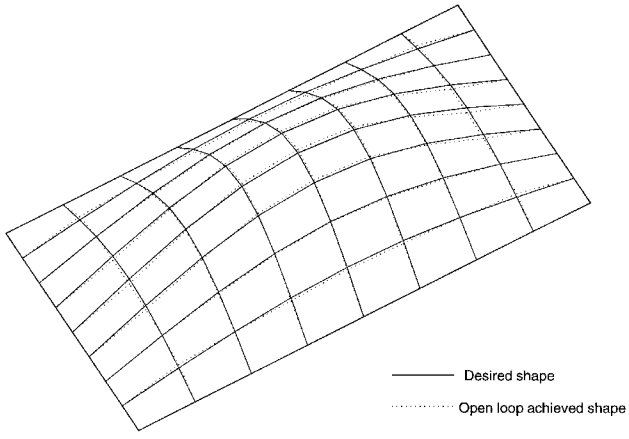

Fig. 8 Three-dimensional view of the desired and open-loop achieved shapes for an SS rectangular plate.

plate dimensions are $a = 0.508$ m, $b = 0.254$ m, and $h = 2.54 \times 10^{-3}$ m. Noncontacting position sensors are used for the purpose of measuring the feedback errors. The sensor output is used to calculate the closed-loop actuator voltages in the presence of quasistatically varying loads. The actuator voltage limit is taken as $-200 < v_i < 200$ V. The plate is modeled by 4×4 full mesh.

Figure 7 shows the open-loop and closed-loop shapes of the plate. The desired shape function is assumed as $w_d = 0.25 \sin(2\pi x/a) \sin(2\pi y/b)$ in millimeters. The open-loop achieved shape is the shape achieved in the absence of unknown external loads. The unknown external load is simulated by applying a uniform load of 200 N/m^2. This unknown external load deforms the open-loop achieved shape into an open-loop distorted shape, as shown in Fig. 7. The mismatch between the desired shape and the distorted shape results in a sensor output error, which is fed back through the shape control gain matrix so as to correct the actuator voltages and, hence, the distorted shape. For this problem full sensor feedback was used. Full sensor feedback means that the nodal displacements of all nodes are measured by the position sensors and fed back to calculate the adaptive voltages. The closed-loop adapted shape, the desired shape, and the open-loop achieved shape match very well. A three-dimensional view of the desired and open-loop achieved shapes is shown in Fig. 8.

Conclusions

An optimal solution to the shape control problem for laminated composite plates is developed using piezoelectric actuators and position sensors. An initial set of optimal actuator voltages is obtained such that a measure of the mean-squared error between the desired and achieved shapes is minimized. A closed-loop control strategy is proposed to minimize the distortion effects due to quasistatically varying loads on the structure. The effectiveness of the algorithm is shown using suitable examples.

References

[1] Lee, C. K., "Theory of Laminated Piezoelectric Plates for the Design of Distributed Sensors/Actuators. Part I: Governing Equations and Reciprocal Relationships," *Journal of the Acoustical Society of America*, Vol. 87, No. 3, 1990, pp. 1144–1158.

[2] Crawley, E. F., and Lazarus, K. B., "Induced Strain Actuation of Isotropic and Anisotropic Plates," *AIAA Journal*, Vol. 29, No. 6, 1991, pp. 944–951.

[3] Wang, B.-T., and Rogers, C. A., "Laminate Plate Theory for Spatially Distributed Induced Strain Actuators," *Journal of Composite Materials*, Vol. 25, Jan. 1991, pp. 433–452.

[4] Chandrashekhara, K., and Agarwal, A. N., "Active Vibration Control of Laminated Composite Plates Using Piezoelectric Devices: A Finite Element Approach," *Journal of Intelligent Material Systems and Structures*, Vol. 4, Oct. 1993, pp. 496–508.

[5] Baz, A., Chen, T., and Ro, J., "Shape Control of Nitinol-Reinforced Composite Beams," *Proceedings of the SPIE Smart Structures and Materials Conference* (Orlando, FL), Vol. 2190, International Society for Optical Engineering, Bellingham, WA, 1994, pp. 436–453.

[6] Austin, F., Rossi, M. J., Nostrand, W. V., and Knowles, G., "Static Shape Control of Adaptive Wings," *AIAA Journal*, Vol. 32, No. 9, 1994, pp. 1895–1901.

[7] Koconis, D. B., Kollar, L. P., and Springer, G. S., "Shape Control of Composite Plates and Shells with Embedded Actuators. I. Voltage Specified," *Journal of Composite Materials*, Vol. 28, No. 5, 1994, pp. 415–457.

A. D. Belegundu
Associate Editor